BULLETIN OF THE POLISH ACADEMY OF SCIENCES
TECHNICAL SCIENCES, Vol. 69(2), 2021, Article number: e136745
DOI: 10.24425/bpasts.2021.136745

Influence of mechanical alloying process on structural, mechanical and tribological behaviours of CNT reinforced aluminium composites – a statistical analysis

P. MANIKANDAN*, A. ELAYAPERUMAL, and R. FRANKLIN ISSAC

Department of Mechanical Engineering, College of Engineering Guindy, Anna University, Chennai – 600025, Tamil Nadu, India

Abstract. The mechanical and tribological properties of the Al/CNT composites could be controlled and improved by the method of its fabrication process. This research article deals with the optimization of mechanical and tribological properties of Al/CNT composites, which are fabricated using the mechanical alloying process with the different weight percentage of multi-walled CNT reinforcement. The phase change and the presence of CNT are identified using the X-Ray Diffraction (XRD) analysis. The influence of mechanical alloying process and the multi-walled CNT reinforcement on the mechanical, and tribological behaviours of the Al/CNT composites are studied. The optimal mechanical alloying process parameters and the weight percentage of multi-walled CNT reinforcement for the Al/CNT composite are identified using the Response Surface Methodology (RSM), which exhibits the better hardness, compressive strength, wear rate and Coefficient of Friction (CoF). The Al/CNT composite with 1.1 wt.% of CNT has achieved the optimal responses at the milling speed 301 rpm and milling time 492 minutes with the ball to powder weight ratio 9.7:1, which is 98% equal to the experimental result. This research also reveals that the adhesive wear is the dominant wear mechanism for the Al/CNT composite against EN31 stainless steel but the optimal Al/CNT composite with 1.1 wt.% of multi-walled CNT has experienced a mild abrasive wear.

Key words: powder metallurgy; composites; morphology; optimization; wear.

1. Introduction

The fabrication process and the pre/post treatment process of metals or Metal Matrix Composites (MMCs) defines its structural and mechanical behaviours [1]. The strength and surface properties of the MMC are improved by the addition of reinforcement, and bulk/surface modification techniques [2–4]. Aluminium (Al) based MMC are generally fabricated using the liquid metallurgy for bulk/mass production [5]. While considering the micro level Al products, the powder metallurgy route plays a major role in achieving the homogenous behaviour and the better mechanical properties with a less material wastage [6]. One of the simple and effective powder metallurgy technique for the fabrication of Al composites is the mechanical alloying process [7].

From previous literature, it is reported that the mechanical alloying process parameters could influence the mechanical properties of Al and its composites. Earlier researchers had experimented the effects of milling parameters on powders and suggested the most influencing factors are milling time, Ball To Powder Ratio (BTPR) and milling speed [8, 9]. Fogagnolo *et al.* [10] studied the effects of mechanical alloying process on microstructure and mechanical properties of the Al and its composites. From the study, it is inferred that the milling time influences the particle size and homogenous distribution. Longer milling time along with the hard reinforcement could increase the hardness of the Al composite. Awotunde *et al.* [11] has done a survey to explore the effects of sintering conditions on the mechanical property of Al and its composites. It concludes that the maximum sintering temperature for the conventional sintering process is 600° for Al composites and the Al composites attains better mechanical property at an optimum sintering temperature of 500°.

Many researchers have reinforced the SiO_2, TiO_2, SiC, TiC, B_4C, TiB_2, BN, CNT and/or Al_2O_3 to the Al alloys for improving their mechanical strength [12, 13]. The addition of low-density reinforcement helps to suit the Al composites for the lightweight systems [14]. The commonly preferred low-density reinforcement for the Al composite is Carbon Nano Tubes (CNT) [15]. The addition of higher wt.% of CNT to the Al matrix will lead to agglomeration, which is due to the high van der Waals force of CNTs [16]. Bunakov *et al.* [17] fabricated the Al/CNT composite using the powder metallurgy technique, in which the same phenomenon is inferred for the addition of 1 wt.% of CNT particles to the Al matrix.

Popov *et al.* [18] carried out an *in-situ* study on the fabrication of Al composites using the mechanical alloying process. This study had revealed that the identification of optimal composition of reinforcement to the matrix is necessary to avoid the intensified mixture in mechanical alloying process. The selection of effective optimization methodology will support to identify the optimal wt.% of reinforcement to the matrix and the optimal fabrication condition for the MMCs [19, 20]. The op-

*e-mail: p.manikandan26@yahoo.com

Manuscript submitted 2020-08-07, revised 2020-12-30, initially accepted for publication 2021-02-11, published in April 2021

timization methodology needs to support the study of intervals of each factor. In this aspect, Response Surface Methodology (RSM) aids to identify the impact of intervals on the response.

Saravanan *et al.* [21] optimized the wear parameters, in which it is stated that the RSM optimization technique explores the responses between the levels of factors through the regression models. This methodology identifies the optimal responses and their influencing factors effectively. Bastwros *et al.* [22] discussed the wear behaviour of Al/CNT composites for the different wt.% of CNT reinforcements. Similarly, Abdullahi *et al.* [23] also discussed the same and mapped the wear mechanism against the wear parameters.

The fabrication process could control the mechanical and tribological properties of the Al/CNT composite, which have been proven by the earlier studies. From available literature, to the best of our knowledge, very few research studies are focused on the effect of controlling factors on the mechanical and tribological properties of the Al/CNT composites. It is also inferred that no detailed systematic analysis to optimize the mechanical alloyed Al/CNT composite in the aspect of mechanical, and wear behaviours. This makes the aim for the current research work to study the influence of the mechanical alloying parameters and CNT reinforcement on mechanical and tribological properties of the Al/CNT composites. RSM is adopted to optimize influencing factors and their levels with considering the mechanical and wear properties of the Al/CNT composites.

2. Materials and methods

For the current research work, Al powder (purity 99.7%) with an average particle size of 78 μm is purchased from Loba Chemie, India and the multi walled CNT (nominal dia of 20–80 nm and length of 3–8 μm) is purchased from Intelligent Materials Private Ltd., India. The purchased CNT is functionalized using acidic treatment for the activation of hydroxyl group in the walls of CNT [24] and it is ball milled using the tungsten carbide balls to blend with Al for different compositions and milling conditions. The mechanical alloying parameters for Al/CNT composites are selected based on the literature and it is tabulated in Table 1. The milled powders are cold pressed at 500 N/mm^{2}using the hydraulic pressing machine (Fig. 1a) with the steel mould (Fig. 1b) to form the samples of 20 mm dia and 10 mm height (Figs. 1c and 1d). After cold pressing, the samples are sintered at 500°C at the heating rate of 10°C/min for 30 minutes and allowed for natural cooling inside the furnace to avoid environmental impact [25].

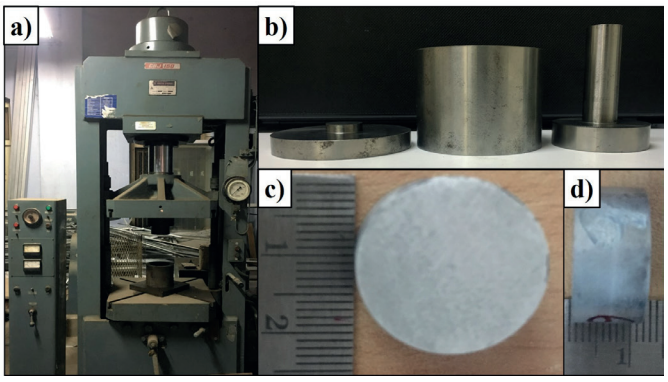

Fig. 1. Photographs of (a) Hydraulic Pressing Machine (b) Mould (c) and (d) Al/CNT sample

Table 1
Parameters of mechanical alloying process for Al/CNT composites

Variable	Factor	Notation	Unit	Range		
				−1	0	+1
A	Material	CNT	wt.%	0	1	2
B	Milling speed	*N*	rpm	250	300	350
C	Milling time	*T*	minutes	240	480	720
D	Ball to powder ratio	BTPR	(x:1)	6	9	12

The fabricated Al/CNT composites are examined using the Field Emission Scanning Electron Microscope (FESEM) and the presence of CNT (carbon) is evidenced through Energy Dispersive x-ray Spectroscopy (EDS) *(Model: SIGMA–ZEISS–Bruker Quantax 200-Z10 EDS)*. The same samples are also examined using the X-Ray Diffractometer (XRD) in Cu-Kα radiation with wavelength of 1.54 Å from the diffraction angle 20° to 90° at a step angle of 0.0° (*Model: X'per PRO*). The XRD patterns are compared with the Joint Committee on Powder Diffraction Standards (JCPDS) and the crystalline structure is studied.

The micro hardness (ASTM B933 – 20) of the fabricated Al/CNT composites is determined using the Vickers micro hardness tester *(Model: Econonet VH – 1D)*, with the load of 300 g for the dwell of 15 s and an average of 5 trails is taken. The compression strength of Al/CNT composites (dia ϕ20 mm, height 10 mm) is evaluated using the automated uniaxial compression testing machine (ASTM B331-16).

The wear study is carried out for the Al/CNT composites using the pin-on-disc tribometer (*Model: DUCOM, TR20LE*) as per the ASTM G99 under dry sliding condition. The dimension of the mechanically alloyed Al/CNT composite pin is machined to dia ϕ6 mm and length of 10 mm and the counterpart steel EN31 disc is machined to dia ϕ55 mm and 10 mm thickness. The wear test is conducted for the applied load 10 N and sliding velocity 1 m/s at the constant sliding distance of 1000 m with the track dia of 40 mm. The mass of the samples is measured before and after wear test using an electronic balancing machine with an accuracy of ±0.0001 g for the determination of wear rate. The friction force is measured by using the load cell; there-by the Coefficient of Friction (CoF) is determined. The worn surface of the Al/CNT composites are examined using the Scanning Electron Microscope (SEM) (*Model: Hitachi S-3400N*).

Based on the selected parameters for mechanical alloying process, the Design of Experiments (DoE) is framed to adopt

the RSM (Box-Behnken Design) to identify the optimal mechanical alloying parameter and CNT reinforcement, which provides the better mechanical and tribological properties for Al/CNT composites. Since the selected factors are four, the design table L_{27} is framed and the responses considered are hardness, compression strength, wear rate and CoF.

3. Results and discussion

3.1. Characterization of mechanical alloyed Al/CNT composites. Figures 2a and 2b evidence the presence of CNT without agglomeration in the Al/CNT composite fabricated using the mechanical alloying condition i.e., 300 rpm milling speed, 480 minutes milling time and 9:1 BTPR. The element composition is analysed by the EDS (Figs. $2a_1$ and $2b_1$), which confirms the percentage of CNT in the composites. The average grain size of the composites is measured, which is 138.2 nm for Al/$CNT_{1\,wt.\%}$ and 173.4 nm for Al/$CNT_{2\,wt.\%}$ composites.

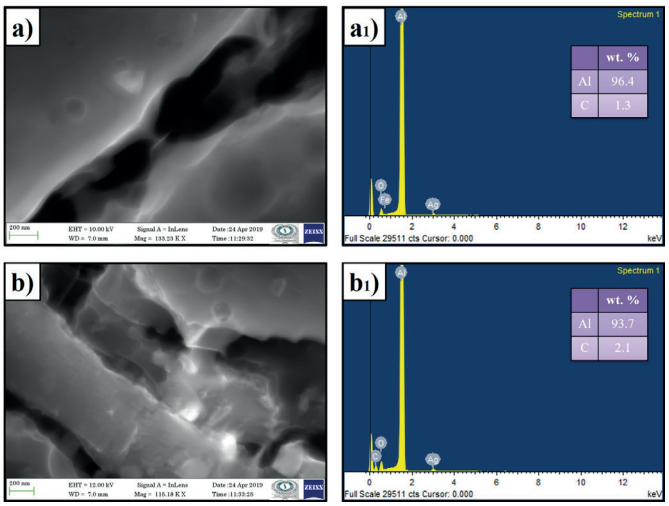

Fig. 2. FESEM of (a) Al/$CNT_{1\,wt.\%}$ composite; (b) Al/$CNT_{2\,wt.\%}$ composite, and EDS of (a_1) Al/$CNT_{1\,wt.\%}$ composite (b_1) Al/$CNT_{2\,wt.\%}$ composite

The mechanical alloying process parameters influence the structural properties of the Al/$CNT_{1\,wt.\%}$ composites, which is evidenced from the SEM images (Fig. 3). This effect will reflect in the mechanical and tribological behaviour of the Al/CNT composites. A laminar structure is visible on the surface of Al/$CNT_{1\,wt.\%}$ composites, the width of the laminar structures is reduced from 5–7 µm (Fig. $3a_1$) to 2–3 µm (Fig. $3a_2$) by the increase the milling speed from 250 to 350 rpm for the milling time of 480 minutes with 9:1 BTPR. This is due to the increase in centrifugal force, which tends to generate a tensile stress along the boundaries of the particles [26].

The average length of the laminar structure observed for the Al/$CNT_{1\,wt.\%}$ composite at the milling time 240 minutes is about 83.2 µm from Fig. $3b_1$ for milling speed 300 rpm with 9:1 BTPR. Similarly, the average length of the laminar structure observed for the Al/$CNT_{1\,wt.\%}$ composite at milling time

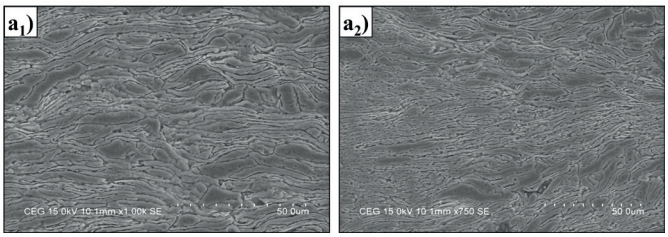

(a) SEM image of Al/$CNT_{1\,wt.\%}$ composites fabricated at milling speed (a_1) 250 and (a_2) 350 rpm for milling time 480 minutes with 9:1 BTPR

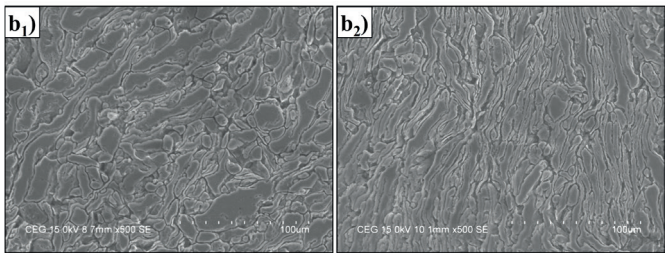

(b) SEM images of Al/$CNT_{1\,wt.\%}$ composites fabricated at milling time (b_1) 240 minutes and (b_2) 720 minutes for milling speed 300 rpm with 9:1 BTPR

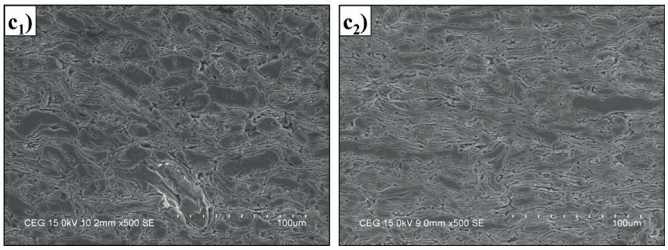

(c) SEM images of Al/$CNT_{1\,wt.\%}$ composites fabricated at BTPR (c_1) 6:1 and (c_2) 12:1 for milling time 480 minutes and milling dpeed 300 rpm

Fig. 3. SEM images of Al/$CNT_{1\,wt.\%}$ composites

720 minutes is about 115.7 µm from Fig. $3b_2$. The prolong milling time had extruded the particles, which is due to the effect of stress mitigation at the boundaries along the centrifugal direction [27].

Figure $3c_1$ shows the irregular and improper formation of particles due to the uneven hammering force created for the less BTPR (6:1) [28]. The same behaviour is not evidenced for the BTPR (12:1) and it provides the equiaxed particles by the effect of milling time 480 minutes and milling speed 300 rpm for the Al/$CNT_{1\,wt.\%}$ composites.

The XRD analysis is carried out for the Al/CNT composites and its patterns are represented in Fig. 4. The peak at 38.47°, 44.72° and 65.09° have the (h,k,l) orientation of (111), (200) and (220), respectively [29], which confirms the Al peaks with a better crystalline nature of the composites (JCPDS card: # 89-2769).

The strong (111) orientation peak is identified at 38.56°, which exhibits the correlation between the grains in the composites i.e., Full Width at Half Maximum (FWHM) phe-

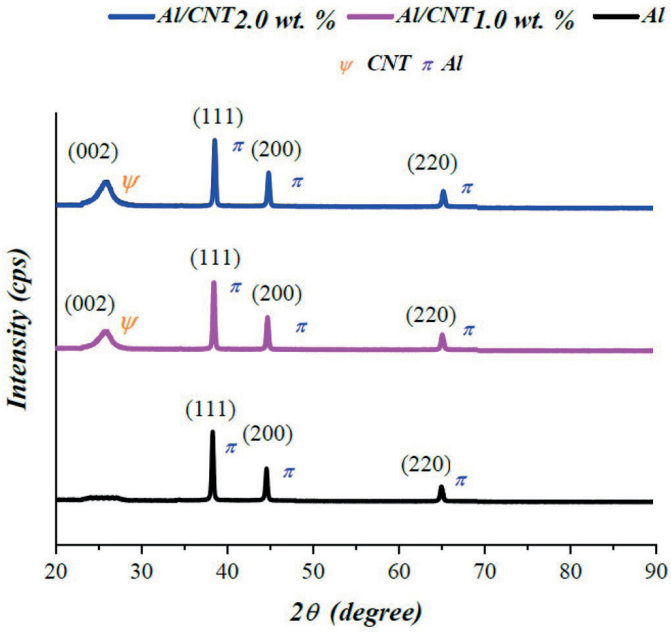

Fig. 4. XRD pattern of Al/CNT composites

nomenon [30]. The XRD pattern reveals the formation of CNT reinforced to the Al matrix from the peak at 26.55° for all the Al/ CNT composites. There is a shift of CNT peak is identified about 0.35° with the lattice (002), when compared to JCPDS (JCPDS card: # 89-8487) of CNT [31]. The CNT peak at 26.55° gets wider from 1 to 2 wt.% of CNT, which may be due to the increase in grain size and it cause grain refinement in the Al/CNT composites.

3.2. Statistical analysis of mechanical alloyed Al/CNT composites. The experiments are conducted based on the design table L_{27} and the results are tabulated in Table 2. All the results tabulated for each run order are the average of three trails.

The normality plot is generated for the residuals of responses. It shows that the residuals of the responses lay on a straight line with a less deviations for regular intervals, which reveals that the samples (trails) are pointed out with a regular non-linear pattern and covering the bounds (levels) of the variables (factors).

Analysis of Variances (ANOVA) is carried out to identify the contribution of influencing factors on responses and to confirm the level of significance. ANOVA for the responses is tabulated in Table 3. The P-Values for all the responses are less than F-Values and 0.05, which shows the level of significance is above 95% [32].

The contribution percentage of models for each response is above 99%, which confirms that all the terms of factors (linear, squares and intermediates terms) are considered in the regression models and also it confirms the best fit of the regression models. The generated second order regression models (uncoded) for the responses is represented in Eqs. (1)–(4). The adequacy of the regression models is tabulated in Table 4 with respected R^2 and $R^2_{(adj)}$, which are above 99% and 98% respectively.

Table 2
Experimental results

Run Order	CNT (wt.%)	Milling speed (rpm)	Milling time (minutes)	BTPR (x:1)	Hardness (HV)	Compression strength (MPa)	Wear rate ($\times 10^{-6}$ g/m)	CoF
1	0	300	240	9	28	49	146	0.38
2	2	350	480	9	31	95	95	0.18
3	2	300	240	9	29	92	101	0.21
4	2	300	480	12	30	94	97	0.19
5	0	250	480	9	23	50	147	0.39
6	1	250	480	12	45	109	79	0.09
7	1	300	720	6	41	103	84	0.12
8	0	300	480	6	22	52	142	0.36
9	2	300	480	6	29	95	99	0.2
10	0	300	720	9	23	51	148	0.4
11	0	350	480	9	24	54	137	0.33
12	0	300	480	12	23	52	144	0.37
13	1	350	480	12	44	108	80	0.1
14	1	300	480	9	46	110	78	0.09
15	1	250	720	9	42	104	84	0.11
16	1	350	240	9	43	107	82	0.1
17	1	300	480	9	46	110	78	0.09
18	1	250	240	9	39	101	87	0.12
19	1	300	240	12	40	99	89	0.13
20	1	350	480	6	41	103	83	0.1
21	1	350	720	9	41	102	85	0.11
22	1	300	480	9	46	110	78	0.09
23	1	300	720	12	42	105	83	0.1
24	1	300	240	6	37	97	90	0.13
25	2	300	720	9	31	95	95	0.18
26	2	250	480	9	32	96	93	0.16
27	1	250	480	6	39	100	88	0.12

$$\begin{aligned} Hardness = {} & -141.7 + 60.33\,CNT + 0.597\,Milling\ Speed \\ & + 0.1285\,Milling\ Time + 0.50\,BTPR - 26.000\,CNT * CNT \\ & - 0.000700\,Milling\ Speed * Milling\ Speed \\ & - 0.000069\,Milling\ Time * Milling\ Time \\ & - 0.3889\,BTPR * BTPR - 0.0100\,CNT * Milling\ Speed \\ & + 0.00208\,CNT * Milling\ Time + 0.083\,CNT * BTPR \\ & - 0.000167\,Milling\ Speed * Milling\ Time \\ & - 0.00833\,Milling\ Speed * BTPR \\ & - 0.00104\,Milling\ Time * BTPR, \end{aligned} \quad (1)$$

$$\begin{aligned}Compression\ Strength = &-125.7 + 96.67CNT \\ &+ 0.640Milling\ Speed + 0.1361Milling\ Time + 9.39BTPR \\ &- 33.667CNT * CNT - 0.000767Milling\ Speed \\ &* Milling\ Speed - 0.000085Milling\ Time * Milling\ Time \\ &- 0.380BTPR * BTPR - 0.0250CNT * Milling\ Speed \\ &+ 0.00104CNT * Milling\ Time - 0.083CNT * BTPR \\ &- 0.000167Milling\ Speed * Milling\ Time \\ &- 0.00667Milling\ Speed * BTPR \\ &- 0.00000Milling\ Time * BTPR, \end{aligned} \quad (2)$$

$$\begin{aligned}Wear\ Rate = &\ 301.2 - 112.83CNT - 0.497Milling\ Speed \\ &- 0.1236Milling\ Time - 9.72BTPR + 39.083CNT * CNT \\ &+ 0.000433Milling\ Speed * Milling\ Speed \\ &+ 0.000093Milling\ Time * Milling\ Time \\ &+ 0.3704BTPR * BTPR + 0.0600CNT * Milling\ Speed \\ &- 0.00833CNT * Milling\ Time - 0.333CNT * BTPR \\ &+ 0.000125Speed * Time + 0.01000Milling\ Speed * BTPR \\ &+ 0.00000Milling\ Time * BTPR, \end{aligned} \quad (3)$$

Table 3
ANOVA for responses

Response	Source	DF	Seq SS	Contribution (%)	Adj SS	Adj MS	F-Value	P-Value
Hardness	Model	14	4685	99.3	4685	334.6	131	0.0
	Error	12	30	0.7	30	2.54		
	Total	26	4716	100				
Compression strength	Model	14	12478	99.5	12478	891.3	177	0.0
	Error	12	60	0.5	60	5.0		
	Total	26	12538	100				
Wear rate	Model	14	16220	99.7	16220	1158.6	272	0.0
	Error	12	51	0.3	51	4.2		
	Total	26	16271	100				
CoF	Model	14	0.3077	99.7	0.3077	0.02197	293	0.0
	Error	12	0.0009	0.3	0.0009	0.00007		
	Total	26	0.3086	100				

Table 4
Adequacy of regression models

Response	R^2	$R^2_{(adj)}$
Hardness	99.35%	98.60%
Compression strength	99.52%	98.96%
Wear rate	99.69%	99.32%
CoF	99.71%	99.37%

$$\begin{aligned}CoF = &\ 0.803 - 0.5300CNT - 0.000867Milling\ Speed \\ &- 0.000382Milling\ Time - 0.0339BTPR \\ &+ 0.17875CNT * CNT - 0.000001Milling\ Speed \\ &* Milling\ Speed + 0.000000Milling\ Time * Milling\ Time \\ &+ 0.001250BTPR * BTPR + 0.000400CNT * Milling\ Speed \\ &- 0.000052CNT * Milling\ Time - 0.00167CNT * BTPR \\ &+ 0.000000Milling\ Speed * Milling\ Time \\ &+ 0.000050Milling\ Speed * BTPR \\ &- 0.000007Milling\ Time * BTPR. \end{aligned} \quad (4)$$

3.3. Influence of mechanical alloying parameters on responses for Al/CNT composites. From Fig. 5, it is observed that the hardness of the Al/CNT composites increases with the increase in CNT reinforcement. The maximum hardness is obtained for the Al/$CNT_{1\,wt.\%}$ composite around 65 HV with the milling time above 480 minutes and the milling speed 300 rpm, which is 1.5 times of the hardness of the Mechanically Alloyed Al. The hardness of the Al/CNT composites is most influenced by CNT about 63.2% and it makes the influence of other factors as insignificant. The influencing order of the factors on hardness of the Al/CNT composites are CNT > milling time > milling speed > BTPR.

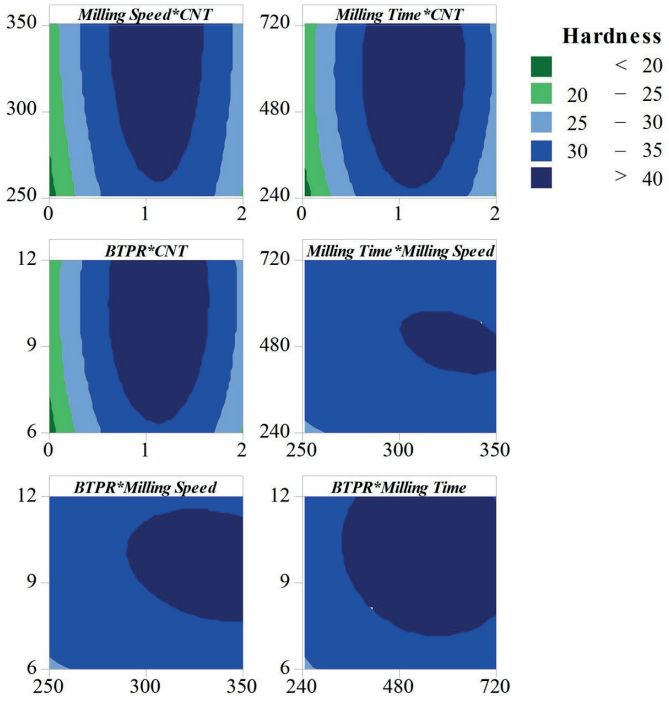

Fig. 5. Hardness of Mechanically Alloyed Al/CNT Composites

The addition of ceramic particles to the Al increases the hardness of the composite [33]. This phenomenon is due to the presence of CNT till 1 wt.% in the Al. Beyond the addition of CNT 1 wt.%, the van der waals force influences the CNT particles to agglomerate [34], which leads to the non-homogenous distribution of reinforcement.

The effect of mechanical alloying process parameters and the CNT in Al/CNT composites on hardness is graphically represented as contour plot in Fig. 6. It is observed that the compression strength of the Al/CNT composites increases with increase in the CNT reinforcement and the maximum compression strength is obtained for Al/$CNT_{1\,wt.\%}$ composite around 110 MPa. The compression strength of the Al/CNT composites is most influenced by CNT about 77.5% and it makes the influence of other factors as insignificant. The influencing order of the factors on compression strength are CNT > milling time > milling speed > BTPR. The addition of CNT increases the interfacial bonding of Al particles, which increases the compression strength of the Al/CNT composite. The addition of CNT more than 1 wt.% decreases the compression strength of the Al/CNT composites due to the ductile to brittle phase transformation [35].

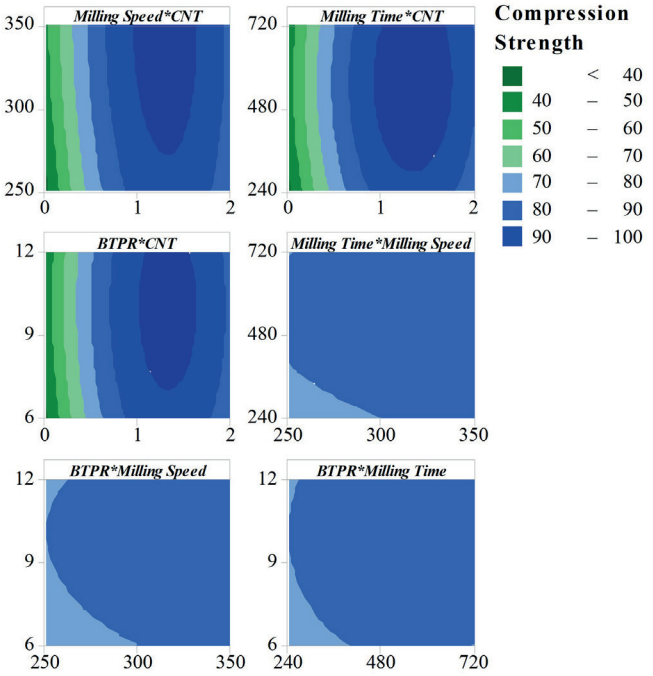

Fig. 6. Compression Strength of Mechanically Alloyed Al/CNT Composites

The minimum wear rate of 78×10^{-6} g/m is obtained for Al/$CNT_{1\,wt.\%}$ composite at the middle level of mechanical alloying parameters. The rate of wear decreases with increase with the CNT reinforcement for Al/CNT composites till 1 wt.% of CNT and thereafter the wear rate is increased minimal till 2 wt.% of CNT (Fig. 7). This phenomenon is due to the cushioning effect [36] of CNT till 1 wt.% and thereafter the CNT starts to flow towards the counterpart.

The wear rate of the Al/CNT composites is highly influenced by CNT and BTPR around 54.1% and 14.7% respectively. The influencing order of the factors on wear rate are CNT > BTPR > milling time > milling speed for the Al/CNT composites. The effect of CNT and mechanical alloying process parameters in Al/CNT composites on CoF is graphically represented

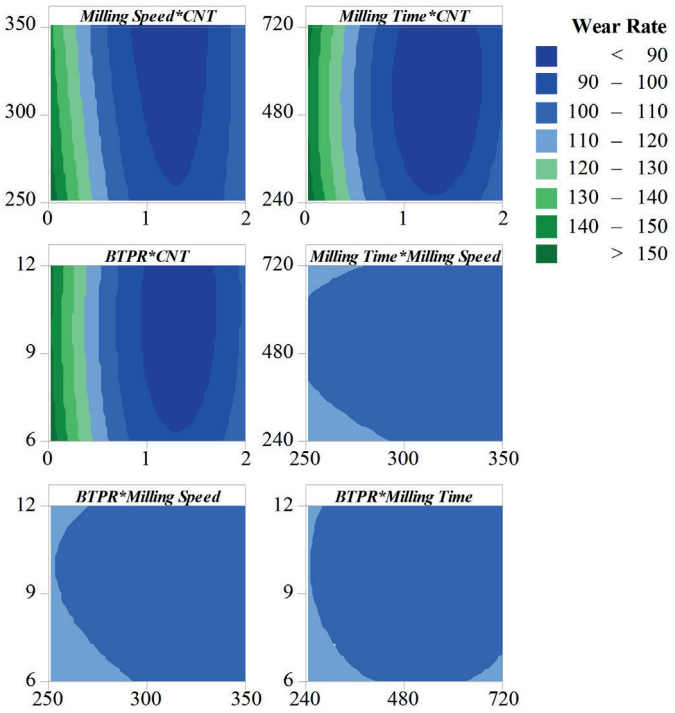

Fig. 7. Wear Rate of Mechanically Alloyed Al/CNT Composites

in Fig. 8. The CoF decrease with increasing the influencing factors till the middle level of it and thereafter the CoF starts to increase by the presence of excess CNT in the Al/CNT composites. The influencing order of the factors on CoF are CNT > milling time > BTPR > milling speed for the Al/CNT composites.

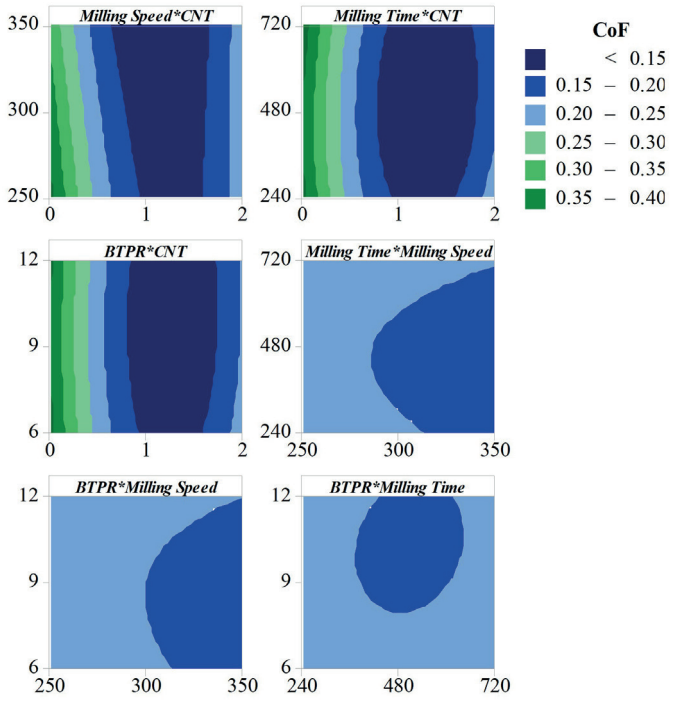

Fig. 8. CoF of Mechanically Alloyed Al/CNT Composites

The CoF of the Al/CNT composites is influenced by all the factors significantly and highly by CNT, milling time and BTPR around 41.2%, 18.8% and 12.6% respectively. The minimum CoF is achieved about 0.09 for the Al/$CNT_{1\,wt.\%}$ composite with milling time of 480 minutes, which is about four times lesser than the mechanically alloyed Al. This effect is because of the self-lubricating behaviour of CNT [37].

3.4. Optimization of mechanical alloying parameters for Al/CNT composites. The optimization is carried out using the RSM technique for the mechanically alloyed Al/CNT composites based on the mechanical and tribological properties and result is represented in Fig. 9.

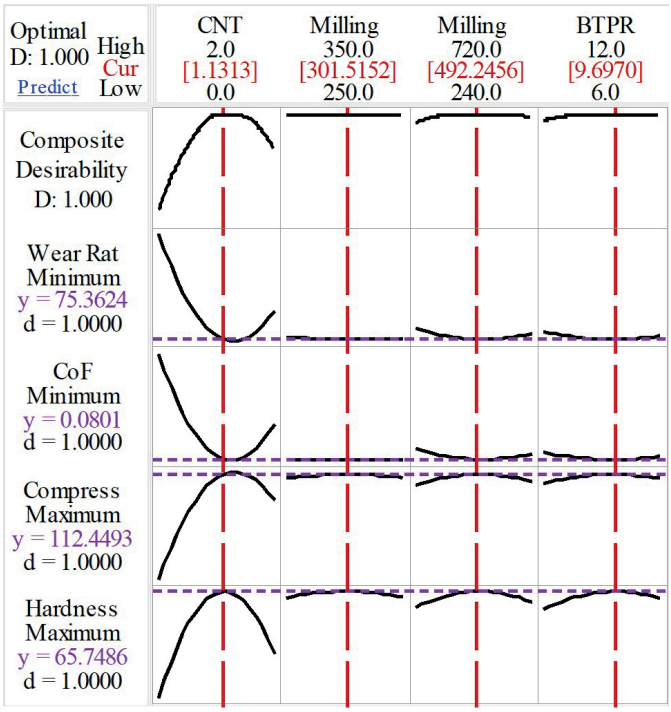

Fig. 9. Optimization plot for mechanically alloyed Al/CNT composite

The optimal response obtained for the Al/$CNT_{1.1\,wt.\%}$ composite at the milling speed of 301.515 rpm, milling time of 492.246 minutes and BTPR of 9.7:1 is tabulated in Table 5. The parent Al, Al/$CNT_{1\,wt.\%}$, Al/$CNT_{2\,wt.\%}$ and optimal Al/$CNT_{1.1\,wt.\%}$ composites are fabricated for the same optimal mechanical alloying condition and the experimental results are tabulated in Table 5. The comparison of theoretical and experimental results shows deviation less than 5%, which confirms the 95% of significance. For the same, the worn surface analysis is carried and represented in Fig. 10. The worn surface of the same parent Al and Al/CNT composites are examined using SEM to study the wear mechanism occurred during the sliding and represented in Fig. 10. A severe adhesive wear is experienced by the parent Al, which is evidenced through Fig. 10a. This is due to the flow of Al pin material to the disc and it sticks on the Al surface, which increases the CoF and tends to increase the wear tremendously.

Table 5
Comparison of results for Al/$CNT_{1.1\,wt.\%}$ composite

Response	Optimal Value		Deviation
	Theoretical	Experimental	
Hardness (HV)	65.749	66.58	1.25%
Compression strength (MPa)	112.45	113.21	0.68%
Wear Rate (g/m)	75.36×10^{-6}	77.069×10^{-6}	2.22%
CoF	0.0801	0.0828	3.26%

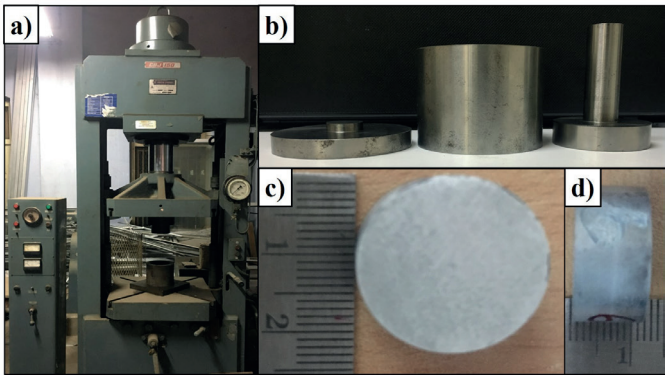

Fig. 10. Worn Surface of (a) Al; (b) Al/$CNT_{1\,wt.\%}$ composite; (c) Al/$CNT_{2\,wt.\%}$ composite and (d) Al/$CNT_{1.1\,wt.\%}$ composite at optimal mechanical alloying condition

A similar behaviour is evidenced in Fig. 10c (Al/$CNT_{2\,wt.\%}$ composite), in which by the presence of CNT particles, the debris is non-sticky so it scratches the Al surface. This is evidenced by the presence of deep grooves on the worn surface of Al/$CNT_{2\,wt.\%}$ composite. In further, the sticky Al debris is fragmented by the CNT debris, which is evidenced by the fragmented surfaces. For Al/$CNT_{1\,wt.\%}$ composite, the presence of debris is lesser, so the formation of grooves is reduced, which is called abrasive wear phenomenon (Fig. 10b) [38]. Figure 10d shows mild abrasive wear for optimal Al/$CNT_{1.1\,wt.\%}$ composite, which results in less wear and friction.

The proper mixture of CNT in Al avoids the loosening of particles during the sliding, which results in the minimal wear and prevents the third body wear mechanism [39,40]. The result of the current study is evidenced from the worn surface analysis and proves that the Al/$CNT_{1.1\,wt.\%}$ composite experiences the optimal wear and friction behaviour compared to the parent Al and Al/CNT composites.

4. Conclusions

- Al/CNT composites are successfully fabricated through the mechanical alloying process with the different wt.% of CNT particles. The homogenous distribution of CNT without agglomeration in the Al/CNT composites is ensured using the FESEM and EDS.

- From the XRD analysis, a shift of CNT peak at 26.55° is identified about 0.35° with the lattice (002) and it gets wider for 2 wt. % of CNT, which may be due to increase in grain size in the Al/$CNT_{2\,wt.\%}$ composite.
- The morphology study reveals that the structure of the particle in the Al/CNT composites is affected by the milling parameters, which confirms the impact of milling parameters in micro level. The impact on grain refinement had increased the hardness and strength of the Al/$CNT_{1\,wt.\%}$ composite about 2 times of the parent Al. Further addition of CNT to the Al had increases the van der waals force and results in agglomeration.
- The minimum wear rate of 78×10^{-6} g/m is obtained for Al/$CNT_{1\,wt.\%}$ composite with the CoF of 0.09, which is almost 4 times lesser than the CoF of mechanically alloyed Al. This phenomenon is due to the self-lubrication behaviour of the CNT particles in the Al/CNT composites.
- The optimal responses are obtained for the Al/$CNT_{1.1\,wt.\%}$ composite at the milling speed of 301 rpm, milling time of 492 minutes and BTPR of 9.7:1 using RSM technique. The comparison of theoretical and experimental results shows deviation less than 5%, which confirms the 95% of significance of models.
- The dominant wear mechanism for the optimal Al/$CNT_{1.1\,wt.\%}$ composite is abrasive wear, which is explored through the SEM images of worn surface study.

Acknowledgements. The corresponding author thanks the University Grants Commission (UGC), India, for providing Rajiv Gandhi National Fellowship (RGNF) (F1-17.1/2016-17/RGNF/2015-17-SC-TAM-7765) to support this work.

References

[1] M.S. Prabhu, A.E. Perumal, S. Arulvel, and R.F. Issac, "Friction and wear measurements of friction stir processed aluminium alloy 6082/$CaCO_3$ composite", *Measurement* 142, 10–20 (2019).

[2] R. Martinez, I. Guillot, and D. Massinon, "New heat treatment to improve the mechanical properties of low copper aluminum primary foundry alloy", *Mater. Sci. Eng.* A 755, 158–165 (2019).

[3] Y. Afkham, R.A. Khosroshahi, S. Rahimpour, C. Aavani, D. Brabazon, and R.T. Mousavian, "Enhanced mechanical properties of in situ aluminium matrix composites reinforced by alumina nanoparticles", *Arch. Civ. Mech. Eng.* 18(1), 215–226 (2018).

[4] J. Li, J. Zhou, Y. Sun, A. Feng, X. Meng, S. Huang, and Y. Sun, "Study on mechanical properties and microstructure of 2024-T351 aluminum alloy treated by cryogenic laser peening", *Optics Laser Tech.* 120, 105670 (2019).

[5] A. Baradeswaran, A. Elayaperumal, and R.F. Issac, "A statistical analysis of optimization of wear behaviour of Al-Al2O3 composites using Taguchi technique", *Procedia Eng.* 64, 973–982 (2013).

[6] P. Sochacka, A. Miklaszewski, and M. Jurczyk, "Development of β-type Ti-x at.% Mo alloys by mechanical alloying and powder metallurgy: Phase evolution and mechanical properties ($10 \leq x \leq 35$)", *J. Alloy. Compd.* 776, 370–378 (2019).

[7] G. Sankaranarayanan, A.N. Balaji, K. Velmanirajan, and K. Gangatharan, "Mechanical and wear behaviour of the Al-Mg-nano ZrC composite obtained by means of the powder metallurgy method", *Bull. Pol. Acad. Sci. Tech. Sci.* 66(5), 729–735 (2018).

[8] A. Canakci, F. Erdemir, T. Varol, and A. Patir, "Determining the effect of process parameters on particle size in mechanical milling using the Taguchi method: measurement and analysis", *Measurement* 46(9), 3532–3540 (2013).

[9] B.L. Tomiczek, A. Dobrzański, and M. Macek, "Effect of milling time on microstructure and properties of AA6061/MWCNTS composite powders", *Arch. Metal. Mater.* 60, 1 (2015).

[10] J.B. Fogagnolo, F. Velasco, M.H. Robert, and J.M. Torralba, "Effect of mechanical alloying on the morphology, microstructure and properties of aluminium matrix composite powders", *Mater. Sci. Eng. A* 342(1-2), 131–143 (2003).

[11] M.A. Awotunde, A.O. Adegbenjo, B.A. Obadele, M. Okoro, B.M. Shongwe, and P.A. Olubambi, "Influence of sintering methods on the mechanical properties of aluminium nanocomposites reinforced with carbonaceous compounds: A review", *J. Mater. Res. Tech.* 8(2), 2432–2449 (2019).

[12] B.P. Kumar and A.K. Birru, "Microstructure and mechanical properties of aluminium metal matrix composites with addition of bamboo leaf ash by stir casting method", *Trans. Nonferrous Met. Soc. China* 27(12), 2555–2572 (2017).

[13] P. Sikder, S. Sarkar, K.G. Biswas, S. Das, S. Basu, and P.K. Das, "Improved densification and mechanical properties of spark plasma sintered carbon nanotube reinforced alumina ceramics", *Mater. Chem. Phys.* 170, 99–107 (2016).

[14] V. Ferreira, P. Egizabal, V. Popov, M.G. de Cortázar, A. Irazustabarrena, A.M. López-Sabirón, and G. Ferreira, "Lightweight automotive components based on nanodiamond-reinforced aluminium alloy: A technical and environmental evaluation", *Diam. Relat. Mat.* 92, 174–186 (2019).

[15] P. Manikandan, R. Sieh, A. Elayaperumal, H.R. Le, and S. Basu, "Micro/nanostructure and tribological characteristics of pressureless sintered carbon nanotubes reinforced aluminium matrix composites", *J. Nanomater.* 2016, 9843019 (2016).

[16] T. Varo, and A. Canakci, "Effect of the CNT content on microstructure, physical and mechanical properties of Cu-based electrical contact materials produced by flake powder metallurgy", *Arab. J. Sci. Eng.* 40(9), 2711–2720 (2015).

[17] N.A. Bunakov, D.V. Kozlov, V.N. Golovanov, E.S. Klimov, E.E. Grebchuk, M.S. Efimov, and B.B. Kostishko, "Fabrication of multi-walled carbon nanotubes–aluminum matrix composite by powder metallurgy technique", *Results Phys.* 6, 231–232 (2016).

[18] V.A. Popov, E.V. Shelekhov, A.S. Prosviryakov, M.Y. Presniakov, B.R. Senatulin, A.D. Kotov, and I.I. Khodos, "Application of nanodiamonds for in situ synthesis of TiC reinforcing nanoparticles inside aluminium matrix during mechanical alloying", *Diam. Relat. Mat.*, 75, 6–11 (2017).

[19] M. Khajelakzay, and S.R. Bakhshi, "Optimization of spark plasma sintering parameters of Si3N4-SiC composite using response surface methodology (RSM)", *Ceram. Int.*, 43(9), 6815 (2017).

[20] K.K. Ekka, and S.R. Chauhan, "Dry sliding wear characteristics of SiC and Al_2O_3 nanoparticulate aluminium matrix composite using Taguchi technique", *Arab. J. Sci. Eng.* 40(2), 571 (2015).

[21] I. Saravanan, A.E. Perumal, R.F. Issac, S.C. Vettivel, and A. Devaraju, "Optimization of wear parameters and their relative effects on TiN coated surface against Ti6Al4V alloy", *Mater. Des.* 92, 23–35 (2016).

[22] M.M. Bastwros, A.M. Esawi, and A. Wifi, "Friction and wear behavior of Al–CNT composites", *Wear* 307(1-2), 164–173 (2013).

[23] U. Abdullahi, M.A. Maleque, and U. Nirmal, "Wear mechanisms map of CNT-Al nano-composite", *Proc. Eng.* 68, 736–742 (2013).

[24] A.M.K. Esawi, K. Morsi, A. Sayed, M. Taher, and S. Lanka, "Effect of carbon nanotube (CNT) content on the mechanical properties of CNT-reinforced aluminium composites", *Compos. Sci. Technol.*, 70(16), 2237–2241 (2010).

[25] C. F. Deng, D.Z. Wang, X.X. Zhang, and A.B. Li, "Processing and properties of carbon nanotubes reinforced aluminum composites", *Mater. Sci. Eng. A* 444(1-2), 138 (2007).

[26] P.R. Soni, *Mechanical alloying: fundamentals and applications*, Cambridge Int. Science Publishing, 2000.

[27] Y. Shi, Z. Ni, Y. Lu, L. Zhao, J. Zou, and Q. Guo, "Interfacial properties and their impact on the tensile behavior of nanolaminated single-walled carbon nanotube-aluminum composite", *Materialia* 12, 100797 (2020).

[28] C. Nie, H. Wang, and J. He, "Evaluation of the effect of adding carbon nanotubes on the effective mechanical properties of ceramic particulate aluminum matrix composites", *Mech. Mater.* 142, 103276 (2020).

[29] Z.Y. Liu, K. Zhao, B.L. Xiao, W.G. Wang, and Z.Y. Ma, "Fabrication of CNT/Al composites with low damage to CNTs by a novel solution-assisted wet mixing combined with powder metallurgy processing", *Mater. Des.* 97, 424–430 (2016).

[30] Z. Hu, F. Chen, J. Xu, Q. Nian, D. Lin, C. Chen, and M. Zhang, "3D printing graphene-aluminum nanocomposites", *J. Alloy. Compd.* 746, 269–276 (2018).

[31] E.A. Belenkov, and F.K. Shabiev, "Scroll structure of carbon nanotubes obtained by the hydrothermal synthesis", *Lett. Mater.* 5(4), 459–462 (2015).

[32] A. Baradeswaran, S.C. Vettivel, A.E. Perumal, N. Selvakumar, and R.F. Issac, "Experimental investigation on mechanical behaviour, modelling and optimization of wear parameters of B4C and graphite reinforced aluminium hybrid composites", *Mater. Des.* 63, 620–632 (2014).

[33] D. Kim, K. Park, K. Kim, T. Miyazaki, S. Joo, S. Hong, and H. Kwon, "Carbon nanotubes-reinforced aluminum alloy functionally graded materials fabricated by powder extrusion process", *Mater. Sci. Eng. A* 745, 379–389 (2019).

[34] C.R. Bradbury, J.K. Gomon, L. Kollo, H. Kwon, and M. Leparoux, "Hardness of multi wall carbon nanotubes reinforced aluminium matrix composites", *J. Alloy. Compd.* 585, 362–367 (2014).

[35] Y. Shi, L. Zhao, Z. Li, Z. Li, D.B. Xiong, Y. Su, and Q. Guo, "Strengthening and deformation mechanisms in nanolaminated single-walled carbon nanotube-aluminum composites", *Mater. Sci. Eng. A* 764, 138273 (2019).

[36] H.J. Choi, S.M. Lee, and D. Bae, "Wear characteristic of aluminum-based composites containing multi-walled carbon nanotubes", *Wear* 270(1-2), 12–18 (2010).

[37] M.A. Xavior, H.P. Kumar, and K.A. Kumar, "Tribological studies on AA 2024–Graphene/CNT Nanocomposites processed through Powder Metallurgy", *Mater. Today Proc.* 5(2), 6588–6596 (2018).

[38] M.R. Akbarpour, S. Alipour, and M. Najafi, "Tribological characteristics of self-lubricating nanostructured aluminum reinforced with multi-wall CNTs processed by flake powder metallurgy and hot pressing method", *Diam. Relat. Mat.*, 90, 93–100 (2018).

[39] Q.M. Gong, Z. Li, Z. Zhang, B. Wu, X. Zhou, Q.Z. Huang, and J. Liang, "Tribological properties of carbon nanotube-doped carbon/carbon composites", *Tribol. Int.* 39(9), 937–944 (2006).

[40] W.S. Im, Y.S. Cho, G.S. Choi, F.C. Yu, and D.J. Kim, "Stepped carbon nanotubes synthesized in anodic aluminum oxide templates", *Diam. Relat. Mat.*, 13(4-8), 1214–1217 (2004).